Journal of Molecular Spectroscopy **210,** 110–118 (2001)
doi:10.1006/jmsp.2001.8436, available online at http://www.idealibrary.com on IDEAL®

Emission Spectroscopy of the $d\,^1\Sigma^+$–$b\,^1\Sigma^+$, $d\,^1\Sigma^+$–$X\,^3\Delta_1$, and $e\,^1\Pi$–$a\,^1\Delta$ Systems of VN

R. S. Ram,* P. F. Bernath,*,† and S. P. Davis‡

*Department of Chemistry, University of Arizona, Tucson, Arizona 85721; †Department of Chemistry, University of Waterloo, Waterloo, Ontario, Canada N2L 3G1; and ‡Department of Physics, University of California, Berkeley, California 94720

Received June 27, 2001; published online October 5, 2001

The emission spectrum of VN has been investigated in the 3400–19 400 cm^{-1} region using a Fourier transform spectrometer. The bands were observed from the reaction of $VOCl_3$ vapor with active nitrogen. In addition to the previously known transitions of VN, several new bands observed in the visible and near infrared have been classified into two new electronic transitions, $e\,^1\Pi$–$a\,^1\Delta$ and $d\,^1\Sigma^+$–$b\,^1\Sigma^+$. Four bands with origins near 5267.49, 5290.48, 5318.86, and 5349.45 cm^{-1} have been identified as the 0–0, 1–1, 2–2, and 3–3 bands, respectively, of the $d\,^1\Sigma^+$–$b\,^1\Sigma^+$ transition. The excited $d\,^1\Sigma^+$ state is known from the $d\,^1\Sigma^+$–$X\,^3\Delta_1$ transition observed previously by B. Simard, C. Masoni, and P. A. Hackett (*J. Mol. Spectrosc.* **136**, 44–55 (1989)). The $d\,^1\Sigma^+$–$X\,^3\Delta_1$ transition has also been observed in our spectra. Another band with two P, two Q, and two R branches and band origin near 14 292.77 cm^{-1} has been assigned as the $e\,^1\Pi$–$a\,^1\Delta$ transition. A rotational analysis of bands of the three transitions has been carried out and the spectroscopic constants have been evaluated. The principal spectroscopic constants for the $a\,^1\Delta$ state, which is most probably the lowest singlet state of VN, are $B_0 = 0.634\,804(31)$ cm^{-1}, $D_0 = 9.03(14) \times 10^7$ cm^{-1}, and $r_0 = 1.554\,891(38)$ Å, while the equilibrium rotational constants for the $b\,^1\Sigma^+$ state are $B_e = 0.617\,896(26)$ cm^{-1}, $\alpha_e = 0.004\,148(19)$ cm^{-1}, and $r_e = 1.576\,022(33)$ Å. The $d\,^1\Sigma^+$ state is affected by interactions with a close-lying perturbing state.

INTRODUCTION

Transition-metal-containing molecules have been the focus of recent investigations because of their importance in astrophysics (*1*), catalysis, and organometallic chemistry (*2–4*). The study of these molecules provides important data needed for the understanding of catalytic processes and chemical bonding in simple metal systems (*3, 4*). Transition metal nitrides, for example, are important in the fixation of nitrogen in industrial, inorganic, and biological systems (*5, 6*). Because of high cosmic abundances of transition metal elements (*7*), several transition-metal-containing diatomic species (oxides and hydrides) have been observed in the spectra of cool M and S type stars (*8–11*). There is a possibility that transition metal nitride molecules may also be found. If detected, their spectra might provide information on the abundance of nitrogen in the atmospheres of cool stars. Precise spectroscopic data on these species are needed for a search. Over the past decade, considerable progress has been made in the characterization of the interaction of transition metal atoms with nitrogen and several theoretical (*12–23*) and experimental studies (*21–31*) have been advanced to achieve this goal.

Among the vanadium-containing molecules, the electronic spectra of VO are the most extensively studied (*32–34*), and the spectra of VN (*35–37*) and VCl (*38*) have also been characterized recently. Peter and Dunn (*35*) observed the emission spectrum of a $^3\Phi - {}^3\Delta$ transition with the 0–0 band near 700 nm, which was labeled as $A^3\Phi$–$X\,^3\Delta$. In the same year, Simard *et al.* (*36*) produced VN in a molecular beam using the laser vaporization technique and observed three transitions, $^3\Phi$–$^3\Delta$, $^3\Pi$–$^3\Delta$, and $^1\Sigma^+$–$^3\Delta_1$ with their 0–0 bands near 700, 624, and 616 nm, respectively. Simard *et al.* (*36*) also obtained a rotational analysis of the 0–0 band of the $^1\Sigma^+$–$^3\Delta_1$ intercombination transition and labeled it $d\,^1\Sigma^+$–$X\,^3\Delta_1$. The 624-nm transition was later studied in a molecular beam source using laser-induced fluorescence by Balfour *et al.* (*37*), who labeled this transition $D\,^3\Pi$–$X\,^3\Delta$. In this work the spectra were recorded at sub-Doppler resolution and the hyperfine structure of the three subbands of the 0–0 band of this transition was observed. Balfour *et al.* (*37*) provided precise rotational and hyperfine constants for the $D\,^3\Pi$ and $X\,^3\Delta$ states.

The reaction of laser-ablated first-row transition metal atoms with N_2 has been investigated by Andrews and co-workers (*39, 40*) and matrix spectra for molecules such as MN and MN_2 have been observed. A sharp VN peak at 1026.2 cm^{-1} observed in solid argon has been assigned as the fundamental vibrational band of VN, in reasonable agreement with the available gas phase value of 1020 ± 5 cm^{-1} (*36*). The spectroscopic properties of the low-lying electronic states of VN have also been calculated recently (*16, 17*). The first calculations were reported by Mattar and Doleman (*16*), who performed multireference CI calculations on a few triplet states of VN while, more recently, Harrison (*17*) has predicted the spectroscopic properties of most of the low-lying singlet and triplet states using MCSCF and multireference CI *ab initio* calculations.

Recently the permanent electric dipole moments in the ground and excited states of VN and CrN have been measured experimentally by Steimle *et al.* (*41*). They have recorded the

0022-2852/01 $35.00

$^3\Pi_0^+$–$X\,^3\Delta_1$, $P(1)$ spectrum of VN and, from the observed Stark splitting, they have obtained a dipole moment of 3.07(7) D for the $X\,^3\Delta_1$ state, compared to the theoretical value of $\mu = 2.77$ D calculated by Harrison (*17*).

In the present investigation we have recorded the emission spectrum of VN in the 3400–19400 cm^{-1} region and have observed two new electronic transitions, $^1\Pi$–$^1\Delta$ and $^1\Sigma^+$–$^1\Sigma^+$, in the singlet manifold, in addition to the transitions observed by previous workers (*35–37*). We have also seen the $d\,^1\Sigma^+$–$X\,^3\Delta_1$ transition of VN, previously observed by Simard *et al.* (*36*). The excited $^1\Sigma^+$ state of our new $^1\Sigma^+$–$^1\Sigma^+$ transition is in common with the excited state of the $d\,^1\Sigma^+$–$X\,^3\Delta_1$ transition. In this paper we will report the rotational analysis of the 0–0, 1–1, 2–2, and 3–3 bands of the $^1\Sigma^+$–$^1\Sigma^+$ transition and the 0–0 bands of the $^1\Pi$–$^1\Delta$ and $d\,^1\Sigma^+$–$X\,^3\Delta_1$ transitions of VN.

EXPERIMENTAL

The VO, VN, and VCl bands were observed in the same experiment from the reaction of flowing $VOCl_3$ vapor and active nitrogen. The details of the experimental setup are provided in our recent paper on VO (*42*). In brief, active nitrogen was produced in a short quartz tube attached to the reaction cell by flowing N_2 through a microwave discharge. The active nitrogen then reacted with $VOCl_3$ vapor introduced at room temperature through another side tube whose inlet was located near the active nitrogen inlet. The intensity of the discharge was controlled by cooling the reaction tube with vapor from liquid nitrogen in a styrofoam container beneath the main reaction tube.

The spectra were recorded with the 1-m Fourier transform spectrometer associated with the McMath–Pierce telescope of the National Solar Observatory at Kitt Peak. The spectra in the interval 3400–19 400 cm^{-1} were recorded in two parts, 3400–14 700 cm^{-1} and 8700–19 400 cm^{-1}, by coadding 29 and 4 scans at a resolution of 0.02 and 0.015 cm^{-1}, respectively. The spectrometer was equipped with a CaF_2 beam splitter. Liquid-nitrogen-cooled InSb and midrange photodiode detectors were used in recording the spectra in the two regions.

In addition to VO, VN, and VCl molecular lines, the spectra also contained CO 2–0 overtone lines present as an impurity. The spectrum was calibrated using the measurements of the 2–0 overtone lines of CO provided by Maki and Wells (*43*). The molecular lines of VN have a typical width of 0.032 cm^{-1} and appear with a maximum signal-to-noise ratio of 8 : 1 so that the best line positions are expected to be accurate to about ± 0.002 cm^{-1}. However, the lines of the $e\,^1\Pi$–$a\,^1\Delta$ transition are frequently overlapped with much stronger lines of the $A\,^3\Phi$–$X\,^3\Delta$ transition; therefore, the uncertainty in the measurement of lines of the $e\,^1\Pi$–$a\,^1\Delta$ transition may be somewhat higher.

LOW-LYING ELECTRONIC STATES OF VN

Three electronic transitions of VN are known to date from the previous analyses of bands observed in the visible region. These transitions were labeled as $A\,^3\Phi$–$X\,^3\Delta$ (*35, 38*), $D\,^3\Pi$–$X\,^3\Delta$ (*37*), and $d\,^1\Sigma^+$–$X\,^3\Delta_1$ (*36*). The electronic structure of VN is expected to be very similar to that of TiO (*44, 45*) and NbN (*46–48*), for which the low-lying electronic states are relatively well characterized and several singlet and triplet states are known experimentally. For VN, however, only the $d\,^1\Sigma^+$ state has been experimentally observed in the singlet manifold. Recent theoretical studies of VN (*17*) predict the presence of several additional low-lying electronic states. For example, a lowest $^3\Sigma^-$ excited state, analogous to the $A\,^3\Sigma^-$ state of NbN (*46–48*), has been predicted in the triplet manifold of VN (*17*). So far this state has not been experimentally observed for TiO. Our present observations provide data for several new low-lying singlet states, $a\,^1\Delta$, $b\,^1\Sigma^+$, and $e^1\Pi$ of VN, consistent with predictions of Harrison (*17*) and available results for TiO (*44, 45*) and NbN (*46–48*). In this paper, therefore, we have taken this opportunity to update the energy level diagram of VN based on our experimental results and the most recent *ab initio* calculations (*17*). The updated energy level diagram of the low-lying electronic states of VN is presented in Fig. 1, where we have labeled the lowest $^3\Sigma^-$ state as $1\,^3\Sigma^-$ and the lowest singlet excited state as $a\,^1\Delta$.

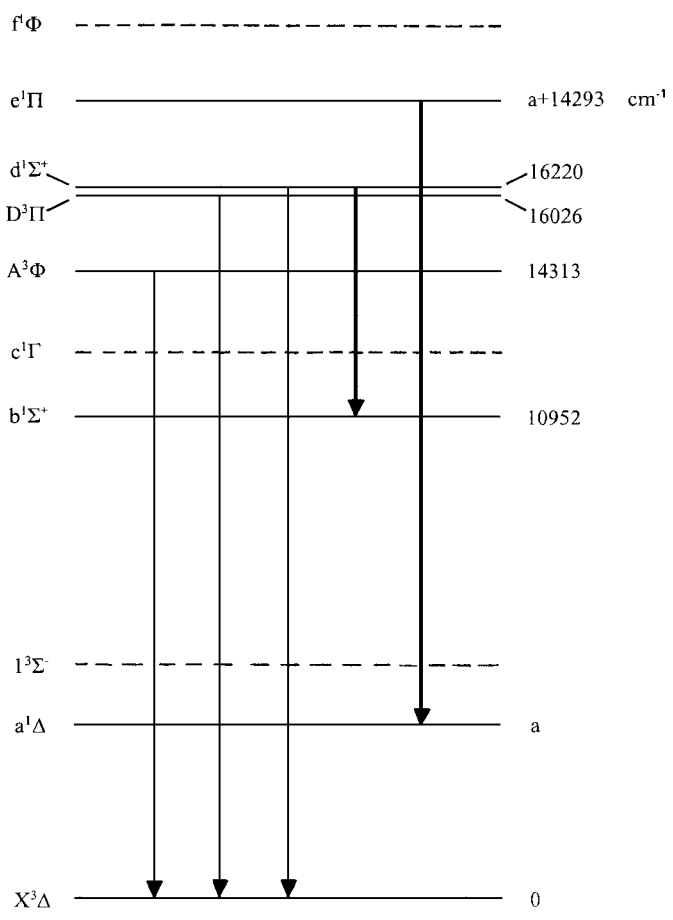

FIG. 1. A schematic energy level diagram for the low-lying electronic states of VN. The new transitions are drawn by bold solid arrows.

The ground state of VN arises from the $3d\delta^1 4s\sigma^1$ configuration (*17, 35–37*), while the $1\,^3\Sigma^-$ and the previously observed $A\,^3\Phi$ and $D\,^3\Pi$ states of VN (Fig. 1) arise from $3d\delta^2$, $3d\delta^1 3\pi^1$, and $3d\delta^1 3\pi^1$ configurations, respectively. In the singlet manifold the ordering of the states is predicted to be $a\,^1\Delta$ ($3d\delta^1 4s\sigma^1$), $b\,^1\Sigma^+$ ($4s\sigma^2$), $c\,^1\Gamma$ ($3d\delta^2$), $d\,^1\Sigma^+$ ($3d\delta^2$), $e\,^1\Pi$ ($3d\delta^1 3d\pi^2$), and $f\,^1\Phi$ ($3d\delta^1 3d\pi^2$). All the singlet electronic states shown in the energy diagram (Fig. 1) were predicted in the *ab initio* calculation of VN by Harrison (*17*), except the c $^1\Gamma$ state. The experimentally observed electronic states of VN have been drawn by solid lines and the states predicted (but not observed yet) have been drawn by broken lines. The previously observed transitions are drawn by normal solid arrows in Fig. 1 while the new electronic transitions observed in this work are drawn by bold solid arrows.

OBSERVATIONS

The spectra were measured using a program called PC-DECOMP developed by J. Brault at Kitt Peak. The peak positions were determined by fitting a Voigt line shape function to each spectral feature and the branches were sorted using a color Loomis–Wood program running on a PC computer. The spectra are full of strong bands belonging to VO and VN. In the region 6000–7300 cm^{-1}, our previously reported [7.0] $^5\Delta$–$X\,^5\Delta$ transition of VCl (*38*) is also present with moderate intensity. In the near infrared a new $1\,^2\Phi$–$1\,^2\Delta$ transition of VO has also been observed for the first time; the analysis will be published elsewhere (*42*). Our Loomis–Wood program was very helpful in identifying the lines, particularly in the weaker and overlapped bands.

Our present spectra consist of a number of new bands of VN in the region 5200–14 400 cm^{-1}, which have been assigned to the $d\,^1\Sigma^+$–$b\,^1\Sigma^+$ and $e\,^1\Pi$–$a\,^1\Delta$ electronic transitions following the notation for the electronic states provided in Fig. 1. The rotational analysis of these two transitions, along with an extended analysis of the $d\,^1\Sigma^+$–$X\,^3\Delta_1$ transition, near 16 220 cm^{-1} (*36*), will be presented in this paper.

(A) The $d\,^1\Sigma^+$–$b\,^1\Sigma^+$ Transition

A group of four bands with open rotational structure has been observed in the region 5200–5400 cm^{-1}. Only bands in the $\Delta v = 0$ sequence have been observed in our spectra. The rotational structure of each band consists of a single R and a single P branch without any doubling, consistent with the $^1\Sigma^+$–$^1\Sigma^+$ assignment.

The lowest wavenumber band with a band origin near 5267 cm^{-1} has been identified as the 0–0 band. This band is slightly weaker in intensity than the 1–1 band and is free from local perturbations, although the effect of interactions in the excited state is reflected by the abnormally large distortion constants. Rotational lines up to $R(38)$ and $P(41)$ have been observed in this band.

The next band with an origin near 5290 cm^{-1} has been identified as the 1–1 band of the $d\,^1\Sigma^+$–$b\,^1\Sigma^+$ transition. A part of the 1–1 band is presented in Fig. 2, in which some P lines have been marked. The rotational lines up to $R(56)$ and $P(56)$ have been identified in this band, which is also free from local perturbations. The next two higher wavenumber bands, with their origins near 5319 and 5349 cm^{-1}, have been identified as the 2–2 and 3–3 bands of the $d\,^1\Sigma^+$–$b\,^1\Sigma^+$ transition. These bands are affected by local perturbations in the excited state near $J' = 27$ and 20, respectively.

A comparison of the rotational constants from the analysis of the 0–0 band of the $d\,^1\Sigma^+$–$b\,^1\Sigma^+$ transition with the constants of the $v = 0$ vibrational level of the $d\,^1\Sigma^+$ state indicates that this transition has an excited state in common with the $d\,^1\Sigma^+$–$X\,^3\Delta_1$ transition.

(B) The $d\,^1\Sigma^+$–$X\,^3\Delta_1$ Transition

The 0–0 band of the $d\,^1\Sigma^+$–$X\,^3\Delta_1$ transition is located near 16 220 cm^{-1}. This transition was previously measured by Simard *et al.* (*36*) by laser-induced fluorescence in a molecular beam and was named the $d\,^1\Sigma^+$–$X\,^3\Delta_1$ transition. We will retain this notation. This transition consists of single R, P, and Q branches with the Q branch being the strongest in intensity.

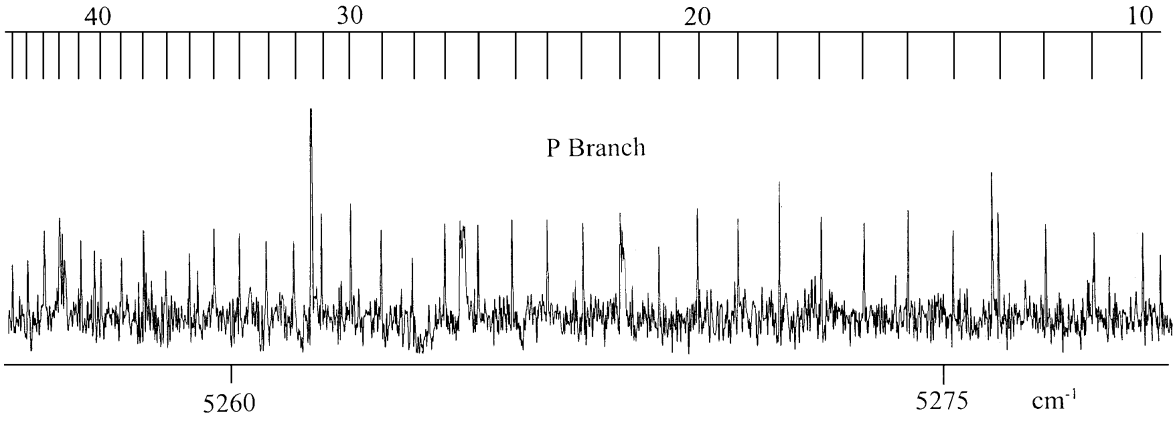

FIG. 2. An expanded portion of the 1–1 band of the $d\,^1\Sigma^+$–$b\,^1\Sigma^+$ transition of VN near the P head.

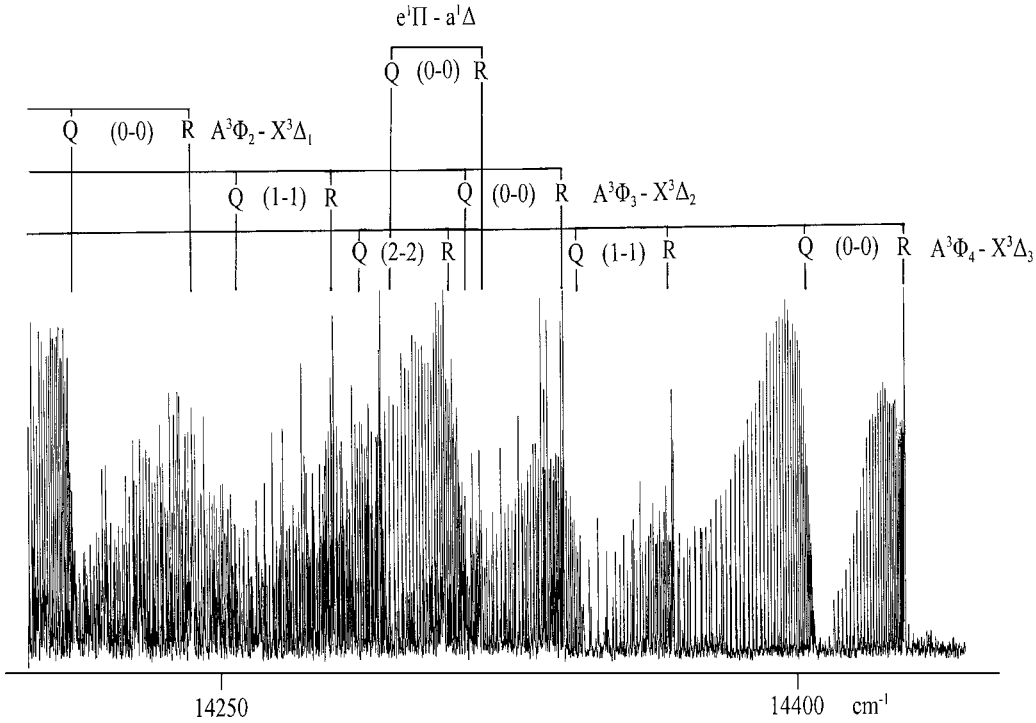

FIG. 3. A compressed portion of the spectrum in the region of the $A\,^3\Phi$–$X\,^3\Delta$ transition of VN with the heads of the $e\,^1\Pi$–$a\,^1\Delta$ transition marked.

Because of the similar magnitudes of the rotational constants in the upper and lower states, this transition also has an open structure and all of the Q lines are piled up in a narrow region of about four wavenumbers. Our measurements of the rotational lines of this transition agree well with the measurements of Simard *et al.* (*36*) within the experimental uncertainty. In our work we have extended the observations to include the lines up to $R(26)$, $P(27)$, and $Q(31)$ of the 0–0 band compared to $R(17)$, $P(21)$, and $Q(21)$ observed in the previous analysis. No other vibrational bands have been identified because of their very weak intensity.

(C) The $e\,^1\Pi$–$a\,^1\Delta$ Transition

The 0–0 band of the $e\,^1\Pi$–$a\,^1\Delta$ transition has Q and R heads near 14 293 and 14 317 cm^{-1}, respectively. This band is heavily overlapped by bands of the strong $A\,^3\Phi$–$X\,^3\Delta$ transition. At first glance (Fig. 3) the $e\,^1\Pi$–$a\,^1\Delta$ transition is not obvious in our spectra. The Loomis–Wood program was again very helpful in identifying this transition, in spite of heavy overlapping. The 0–0 band consists of two R, two P, and two Q branches with negligible Λ-doubling in the lower state. This transition has been assigned as the $e\,^1\Pi$–$a\,^1\Delta$ transition of VN. The 1–1 and other higher vibrational bands could not be identified because of their weaker intensity and strong overlapping from the bands of the $A\,^3\Phi$–$X\,^3\Delta$ transition. A part of the compressed spectrum of VN in the $e\,^1\Pi$–$a\,^1\Delta$ region is presented in Fig. 3, with the Q and R heads marked.

No off diagonal bands of the $d\,^1\Sigma^+$–$b\,^1\Sigma^+$, $d\,^1\Sigma^+$–$X\,^3\Delta_1$, and $e\,^1\Pi$–$a\,^1\Delta$ transitions of VN have been observed in our spectra, so none of the vibrational intervals of the singlet electronic states could be determined.

RESULTS AND DISCUSSION

Although the first lines were generally not identified, there is no doubt in the assignment of the $d\,^1\Sigma^+$–$b\,^1\Sigma^+$ transition because the upper state is common to the singlet–triplet intercombination transition measured by Simard *et al.* (*36*). The rotational analysis of the $e\,^1\Pi$–$a\,^1\Delta$ transition is secure because of the presence of Q branches. The observed line positions of the $d\,^1\Sigma^+$–$b\,^1\Sigma^+$, $d\,^1\Sigma^+$–$X\,^3\Delta_1$, and $e\,^1\Pi$–$a\,^1\Delta$ transitions of VN are provided in Table 1. The molecular constants were determined by fitting the observed line positions with the customary energy level expressions:

(for $^1\Sigma^+$, $^1\Delta$, and $^3\Delta_1$ states)

$$F_v(J) = T_v + B_v J(J+1) - D_v[J(J+1)]^2 + H_v[J(J+1)]^3 \quad [1]$$

(for $^1\Pi$ state)

$$F_v(J) = T_v + B_v J(J+1) - D_v[J(J+1)]^2 + H_v[J(J+1)]^3 \pm 1/2[q_v J(J+1) + q_{Dv}(J(J+1))^2]. \quad [2]$$

TABLE 1

Observed Line Positions (in cm^{-1}) for the $d\ ^1\Sigma^+–b\ ^1\Sigma^+$, $d\ ^1\Sigma^+–X\ ^3\Delta_1$, and $e\ ^1\Pi–a\ ^1\Delta$ Transitions of VN

J	R(J)	O-C	P(J)	O-C	R(J)	O-C	P(J)	O-C	R(J)	O-C		P(J)	O-C	
	$d^1\Sigma^+ - b^1\Sigma^+$ 0-0				$d^1\Sigma^+ - b^1\Sigma^+$ 1-1				$d^1\Sigma^+ - b^1\Sigma^+$ 2-2					
2			5265.051	3					5322.627	2				
3	5272.628	1	5263.862	3			5286.873	6	5323.912	-7		5315.281	5	
4	5273.961	-2	5262.688	-2	5296.892	0	5285.699	-4	5325.234	1		5314.121	1	
5	5275.317	-1	5261.538	-5	5298.239	6	5284.562	2	5326.569	3		5312.985	1	
6	5276.689	-4	5260.411	-5	5299.603	7	5283.439	3	5327.926	7		5311.873	4	
7			5259.308	-1	5300.981	4	5282.332	-0	5329.291	0		5310.776	4	
8	5279.499	-1	5258.221	-1	5302.380	1	5281.249	0	5330.681	-0		5309.686	-10	
9	5280.931	0	5257.155	1	5303.802	2	5280.185	0	5332.093	2		5308.637	-2	
10	5282.378	0	5256.114	8	5305.241	1	5279.142	1	5333.519	-2		5307.603	1	
11	5283.840	-2	5255.073	-2	5306.701	-1	5278.119	1	5334.966	-3		5306.581	-3	
12	5285.319	-1	5254.066	4	5308.181	-0	5277.115	-0	5336.433	-2		5305.585	-1	
13	5286.818	5	5253.070	5	5309.686	6	5276.131	-0	5337.916	-4		5304.605	-2	
14	5288.322	2	5252.089	4	5311.198	-2	5275.168	-1	5339.419	-4		5303.643	-4	
15	5289.840	1	5251.126	7	5312.738	-1	5274.224	-2	5340.941	-3		5302.703	-4	
16	5291.374	4	5250.170	4	5314.295	-2	5273.305	1	5342.482	-1		5301.782	-3	
17	5292.910	-0	5249.230	1	5315.874	-0	5272.401	-0	5344.039	-1		5300.879	-3	
18	5294.460	-0	5248.293	-9	5317.464	-8	5271.521	2	5345.616	2		5299.996	-2	
19	5296.017	-1	5247.388	1	5319.088	-0	5270.657	-1	5347.209	4		5299.138	6	
20	5297.584	0	5246.485	4	5320.721	-4	5269.812	-4	5348.819	5		5298.285	1	
21			5245.585	-0	5322.377	-4	5268.996	1	5350.442	4		5297.460	5	
22	5300.727	-3	5244.696	-1	5324.053	-2	5268.190	-4	5352.082	2		5296.645	2	
23	5302.307	-2	5243.813	-2	5325.747	-3	5267.413	-0	5353.738	-0		5295.852	3	
24	5303.886	-5	5242.936	-3	5327.461	-2	5266.652	-2	5355.407	-4		5295.077	4	
25	5305.474	0	5242.068	-0	5329.195	-1	5265.911	-3	5357.089	-10		5294.314	1	
26	5307.055	-1	5241.200	-1	5330.945	-3	5265.191	-4	5358.775	-28	a	5293.565	-6	
27	5308.637	-1	5240.332	-3	5332.715	-4	5264.497	1	5360.464	-58	a	5292.829	-16	
28	5310.215	-2	5239.469	-1	5334.507	-4	5263.816	-2	5362.146	-109	a	5292.105	-30	a
29	5311.793	0	5238.609	3	5336.310	-10	5263.158	-2	5363.819	-184	a	5291.374	-68	a
30	5313.363	-2	5237.739	-2	5338.157	8	5262.521	-2	5365.440	-325	a	5290.656	-108	a
31	5314.933	2	5236.876	2	5340.001	3	5261.898	-8				5289.915	-187	a
32	5316.496	4	5236.006	2	5341.868	2	5261.319	9				5289.137	-319	a
33	5318.043	-3	5235.134	4	5343.750	-3	5260.739	3						
34	5319.593	0	5234.254	2	5345.660	2	5260.182	2						
35	5321.131	-0	5233.364	-4	5347.580	-4	5259.647	1						
36	5322.665	5			5349.534	7	5259.133	0						
37	5324.180	-2	5231.585	3	5351.495	4	5258.638	-2						
38	5325.693	-1	5230.678	-2	5353.471	-1	5258.176	8						
39			5229.767	-3	5355.477	3	5257.720	3						
40			5228.853	1	5357.499	5	5257.288	2						
41			5227.927	-0	5359.532	-1	5256.879	2						
42					5361.590	-1	5256.488	1						
43					5363.669	1	5256.114	-5						
44					5365.766	1	5255.768	-3						
45					5367.867	-12	5255.449	4						
46					5370.015	1	5255.139	-1						
47					5372.171	6	5254.856	1						
48					5374.335	-2	5254.593	2						
49					5376.523	-5	5254.349	-0						
50					5378.740	4	5254.133	5						
51					5380.961	-4	5253.925	-2						
52					5383.212	1	5253.746	-1						
53							5253.589	0						
54					5387.761	1	5253.449	-3						
55					5390.063	-0	5253.333	-2						
56					5392.382	-2	5253.241	1						

Note. Lines marked by "a" are perturbed lines and O-C are observed minus calculated wavenumbers in units of 10^{-3} cm^{-1}.

TABLE 1—*Contiuned*

J	R(J)	O-C	P(J)	O-C	R(J)	O-C	P(J)	O-C	Q(J)	O-C
	$d^1\Sigma^+ - b^1\Sigma^+$ 3-3				$d^1\Sigma^+ - X^3\Delta_1$ 0-0					
1					16222.707	1			16220.193	-7
2					16223.988	4	16217.719	-2	16220.223	-4
3			5345.890	-2	16225.274	-2	16216.506	-1	16220.263	-2
4			5344.749	4	16226.582	3	16215.302	-5	16220.321	4
5	5357.089	-12	5343.624	7	16227.893	-1	16214.122	3	16220.385	4
6	5358.440	-4			16229.217	-4	16212.944	0	16220.464	7
7	5359.800	-4	5341.422	4	16230.558	-1	16211.771	-8	16220.546	2
8	5361.185	1	5340.350	2	16231.906	1	16210.630	2	16220.640	-2
9	5362.580	-2	5339.303	6	16233.268	6	16209.488	2	16220.749	-0
10	5363.995	-3	5338.261	-5	16234.638	11	16208.366	10	16220.869	1
11	5365.440	7	5337.248	-5	16236.001	0	16207.236	1	16220.999	5
12	5366.884	-0	5336.258	-1	16237.382	2	16206.124	2	16221.138	10
13	5368.350	-3	5335.276	-7	16238.758	-8	16205.027	9	16221.270	1
14	5369.843	3	5334.324	-2	16240.158	2	16203.919	-1	16221.416	-1
15	5371.350	6	5333.386	-1	16241.551	1	16202.830	-0	16221.569	-0
16	5372.869	5	5332.466	1	16242.950	3	16201.739	-6	16221.722	-3
17	5374.402	2	5331.564	3	16244.336	-9	16200.667	3	16221.885	0
18	5375.943	-9	5330.681	6	16245.743	-0	16199.592	7	16222.045	-0
19	5377.459	-60 a	5329.803	-3	16247.149	9	16198.517	8	16222.201	-6
20	5378.968	-134 a	5328.940	-12	16248.533	-3	16197.445	11	16222.381	13
21			5328.050	-66 a	16249.921	-6	16196.356	-2	16222.524	-2
22					16251.312	-1	16195.291	10	16222.684	3
23	5384.411	477 a			16252.692	-2	16194.198	-2	16222.832	-0
24	5386.045	474 a			16254.067	0	16193.117	1	16222.985	8
25	5387.720	500 a	5325.396	473 a	16255.432	1	16192.028	2	16223.122	7
26	5389.431	548 a	5324.630	469 a	16256.788	4	16190.935	6	16223.253	8
27	5391.164	608 a	5323.912	498 a			16189.819	-6	16223.374	10
28	5392.914	674 a	5323.220	540 a					16223.488	15
29	5394.686	751 a	5322.560	603 a					16223.565	-5
30	5396.470	830 a	5321.923	676 a					16223.655	2
31	5398.272	920 a	5321.297	748 a					16223.719	-3
32			5320.721	859 a						
33	5402.057	1254 a	5320.150	965 a						
34	5403.915	1376 a	5319.593	1075 a						
35	5405.804	1522 a	5319.088	1228 a						
36	5407.722	1692 a	5318.583	1372 a						
37	5409.654	1871 a	5318.094	1525 a						
38			5317.621	1686 a						
39			5317.174	1866 a						
40			5316.741	2056 a						
41			5316.336	2268 a						

J	R_{ee}(J)	O-C	P_{ee}(J)	O-C	R_{fl}(J)	O-C	P_{fl}(J)	O-C	Q_{ef}(J)	O-C	Q_{fe}(J)	O-C
					$e^1\Pi - a^1\Delta$ 0-0							
5	14299.725	-12			14299.725	7			14292.291	-14	14292.291	-0
6	14300.790	1	14284.702	14	14300.790	26			14292.103	-16	14292.103	3
7	14301.785	-26	14283.217	-16	14301.785	7	14283.217	2	14291.882	-22	14291.882	3
8	14302.758	-44 a	14281.728	-20	14302.758	-4 a	14281.728	5	14291.637	-20	14291.637	13
9			14280.207	-25 a			14280.207	7				
10	14304.708	18			14304.649	18						
11					14305.539	21			14290.747	18	14290.688	18
12	14306.455	1			14306.376	4			14290.366	8	14290.298	9
13	14307.284	-5	14273.871	10	14307.169	-26	14273.804	12	14289.959	3	14289.882	6
14	14308.106	14	14272.186	-6	14307.984	-2	14272.109	-2	14289.523	-1	14289.434	3
15	14308.858	-8	14270.493	0	14308.742	-2	14270.404	5	14289.057	-4	14288.953	-1
16	14309.603	-4	14268.760	-2	14309.489	18	14268.645	-10	14288.556	-10	14288.443	-2
17	14310.324	7					14266.873	-7	14288.044	3		
18	14310.991	-4	14265.219	10	14310.832	5			14287.495	10	14287.345	12

TABLE 1—*Contiuned*

J	R_{ee}(J)	O-C	P_{ee}(J)	O-C	R_{ff}(J)	O-C	P_{ff}(J)	O-C	Q_{ef}(J)	O-C	Q_{fe}(J)	O-C
						$e^1\Pi$ - $a^1\Delta$ 0-0						
19	14311.639	-4	14263.403	15	14311.451	-5	14263.248	12	14286.901	4	14286.725	-4
20	14312.254	-5	14261.538	4	14312.049	-5	14261.374	8	14286.279	-1	14286.099	6
21	14312.827	-16	14259.650	-1	14312.609	-10	14259.467	2	14285.625	-5	14285.423	-2
22	14313.346	-49 a	14257.734	-4	14313.108	-43 a	14257.530	-3	14284.932	-18 a	14284.702	-24 a
23	14313.971	54 a	14255.782	-11			14255.562	-7	14284.191	-47 a	14283.968	-26 a
24	14314.416	11	14253.784	-33 a	14314.135	16	14253.545	-29 a	14283.551	55 a	14283.217	-14
25	14314.873	11	14251.868	56 a	14314.564	11			14282.733	12	14282.453	17
26			14249.793	18	14314.952	-4	14249.508	19	14281.921	5	14281.609	1
27	14315.666	-14	14247.712	4	14315.322	-3	14247.404	5	14281.074	-5	14280.751	4
28	14316.034	-7	14245.613	3	14315.666	6	14245.280	2	14280.207	-4	14279.854	-1
29	14316.326	-43 a	14243.479	-1	14315.936	-27 a	14243.122	-3	14279.298	-13	14278.927	-3
30	14316.662	-2	14241.311	-9	14316.246	14	14240.935	-4	14278.346	-33 a	14277.943	-29 a
31	14316.931	4	14239.091	-37 a	14316.470	3			14277.420	6	14276.992	10
32	14317.154	-2	14236.917	12	14316.662	-6	14236.478	6	14276.431	13	14275.958	-0
33	14317.358	6	14234.651	0	14316.835	-1	14234.180	-11	14275.386	-2	14274.899	-3
34	14317.512	-1	14232.363	-1			14231.873	-3	14274.322	-5	14273.804	-7
35	14317.649	8	14230.043	-3	14317.045	-22	14229.532	2	14273.228	-5	14272.683	-4
36			14227.699	5			14227.131	-19	14272.109	5	14271.525	-5
37			14225.300	-12			14224.731	-6	14270.934	-8	14270.332	-5
38			14222.900	4			14222.288	-2	14269.747	0	14269.109	-1
39			14220.457	10			14219.813	3	14268.518	1	14267.830	-18
40			14217.947	-17			14217.290	-5	14267.257	5	14266.554	3
41			14215.447	-1			14214.755	8	14265.959	7	14265.219	1
42			14212.901	4			14212.169	6	14264.624	6	14263.853	3
43			14210.318	6			14209.552	8	14263.248	1	14262.445	2
44							14206.894	5	14261.841	3	14261.004	4
45									14260.388	-5	14259.521	2
46									14258.900	-9	14257.991	-9

In the final fit the blended lines were given a reduced weighting and badly overlapped lines were excluded in order to improve the standard deviation of the fit. The perturbed lines in the 2–2 and 3–3 bands of the $d\,^1\Sigma^+$–$b\,^1\Sigma^+$ transition were also heavily deweighted. The bands of the $d\,^1\Sigma^+$–$b\,^1\Sigma^+$ and $d\,^1\Sigma^+$–$X\,^3\Delta_1$ transitions were initially fitted separately but in the final fit the 0–0 bands of the two transitions were combined to determine a single set of molecular constants for the $v = 0$ vibrational level of the $d\,^1\Sigma^+$ state. We have observed additional higher J lines in the $d\,^1\Sigma^+$–$X\,^3\Delta_1$ transition than previously reported by Simard *et al.* (*36*) and this has provided improved constants for the $d\,^1\Sigma^+$ state. The molecular constants obtained from the final fits are provided in Table 2.

The carrier of the new bands was established on the basis of the experimental evidence and by comparison with the known spectra of VO, VN, and VO^+. The magnitude of the B values of the observed states was very helpful in making a definite identification. The upper and lower states of the new transitions reported here are fitted as odd multiplicity states and their B values are >0.61 cm^{-1}, while the VO states have even multiplicity with B values of $\sim$0.55 cm^{-1}. The B values of our new transitions are also inconsistent with the VO^+ molecule, for which two singlet transitions have been observed with B values of the order of $\sim$0.53 cm^{-1} (*49*). The electronic spectra of VC are not known yet and it is very unlikely that this molecule would have formed under our experimental conditions. Moreover, the new near infrared transition at 5267 cm^{-1} has an excited state in common with the $d\,^1\Sigma^+$–$X\,^3\Delta_1$ transition VN, first observed by Simard *et al.* (*36*). This removes any doubt about the identity of the carrier of the new infrared bands. The 14 293 cm^{-1} band, assigned here as the $e\,^1\Pi$–$a\,^1\Delta$ transition, has upper and lower state B values of 0.62 and 0.64 cm^{-1}, respectively. The states of this transition are also of odd multiplicity and their rotational constants are again too big for molecules like VO and VO^+.

Because off-diagonal bands were not observed in any of the transitions reported in this paper, the vibrational intervals remain unknown for the observed singlet electronic states of VN. However, the observation of the 1–1, 2–2, and 3–3 bands in addition to the 0–0 band of the $d\,^1\Sigma^+$–$b\,^1\Sigma^+$ transition has enabled us to determine equilibrium rotational constants for the $d\,^1\Sigma^+$ and $b\,^1\Sigma^+$ states (Table 3). As can be noted in Table 2, the rotational constants for the $b\,^1\Sigma^+$ state vary relatively smoothly with v, indicating that this state is free from interactions. The rotational constants of Table 2 provide $B_e = 0.617\,896(26)$ cm^{-1}

TABLE 2
Molecular Constants[a] (in cm^{-1}) for VN

State	v	T_v	B_v	$10^6 \times D_v$	$10^{10} \times H_v$	$10^4 \times q_v$	$10^8 \times q_{Dv}$
$e^1\Pi$	0	a+14292.7689(17)	0.619123(33)	0.858(18)	-0.618(29)	4.492(34)	-1.32(22)
	3	d+5349.4533(17)	0.613061(60)	1.77(12)	--	--	--
	2	c+5318.8615(11)	0.617422(37)	1.433(43)	--	--	--
	1	b+5290.47700(61)	0.621621(11)	0.9298(26)	--	--	--
$d^1\Sigma^+$	0	16220.18732(56)	0.626412(14)	4.082(11)	4.048(43)	--	--
	3	d	0.603273(63)	0.939(13)	--	--	--
	2	c	0.607521(37)	0.955(41)	--	--	--
	1	b	0.611683(11)	0.9308(27)	--	--	--
$b^1\Sigma^+$	0	10952.6975(10)	0.615811(14)	0.9249(73)	--	--	--
$a^1\Delta$	0	a	0.634804(31)	0.903(14)	--	--	--
$X^3\Delta_1$	0	0	0.619857(14)	0.6644(92)	-	--	--

[a] Numbers in parentheses are one standard deviation in the last digits quoted.

and $\alpha_e = 0.0041\,48(19)$ cm^{-1} for the $b\,^1\Sigma^+$ state. As has been mentioned previously, the $d\,^1\Sigma^+$ state is affected by interactions with some unknown state (or states). A careful inspection of the constants of Table 2 shows that the $v = 0$, 2, and 3 vibrational levels of the $d\,^1\Sigma^+$ state are affected by these interactions. Although no local perturbations have been observed in the $v = 0$ vibrational level of the $d\,^1\Sigma^+$ state, the distortion constants have unexpectedly large magnitudes. The values of $D_0 = 4.082(11) \times 10^{-6}$ cm^{-1} and $H_0 = 4.048(43) \times 10^{-10}$ cm^{-1} were determined for $v = 0$ and they are an order of magnitude bigger than the values expected for an isolated level of the VN molecule. The effects of interactions are clearly visible in the $v = 2$ and 3 vibrational levels of the $d\,^1\Sigma^+$ state in which local perturbations have been observed at $J = 27$ and 20, respectively. Because of these interactions, the rotational constants for the four ($v = 0$, 1, 2, and 3) vibrational levels vary somewhat irregularly (see Table 2). The constants of Table 2 provide equilibrium rotational constants of $B_e = 0.628\,61(21)$ cm^{-1} and $\alpha_e = 0.004\,59(15)$ cm^{-1} for the $d\,^1\Sigma^+$ state (See Table 3). The equilibrium rotational constants for the $b\,^1\Sigma^+$ and $d\,^1\Sigma^+$ states have been used to calculate the equilibrium bond lengths of 1.576 022(33) and 1.562 53(26) Å, respectively. The theoretical values of $r_e = 1.598$ and 1.632 Å have been obtained for the $d\,^1\Sigma^+$ and $b\,^1\Sigma^+$ states, respectively. For the $a\,^1\Delta$ and $e\,^1\Pi$ states the respective r_0 bond lengths of 1.554 891(38) and 1.574 459(42) Å were obtained experimentally. These values can be compared with the theoretical values of $r_e = 1.596$ Å ($a\,^1\Delta$) and $r_e = 1.594$ Å ($e\,^1\Pi$) obtained by Harrison (*17*).

TABLE 3
Equilibrium Constants (in cm^{-1}) for VN

Constants	B_e	α_e	r_e (Å)
$e^1\Pi$	0.619123(33)[a]	--	1.574459(42)[b]
$d^1\Sigma^+$	0.62861(21)	0.00459(15)	1.56253(26)
$b^1\Sigma^+$	0.617896(26)	0.004148(19)	1.576022(33)
$a^1\Delta$	0.634804(31)[a]	--	1.554891(38)[b]
$X^3\Delta_1$	0.619857(14)[a]	--	1.573527(18)[b]

[a] B_0 values.
[b] r_0 values.

CONCLUSION

The emission spectrum of VN has been investigated in the region extending from the near infrared to the visible using a Fourier transform spectrometer. The new bands observed in the region 5200–14400 cm^{-1} have been assigned to two new electronic transitions, $d\,^1\Sigma^+$–$b\,^1\Sigma^+$ and $e\,^1\Pi$–$a\,^1\Delta$, adopting the notation for the isovalent NbN molecule and the energy level diagram for VN provided in Fig. 1. The $d\,^1\Sigma^+$–$X\,^3\Delta_1$ transition previously observed by Simard *et al.* (*36*) has also been observed. A rotational analysis of the 0–0, 1–1, 2–2, and 3–3 bands of the $d\,^1\Sigma^+$–$b\,^1\Sigma^+$ transition and the 0–0 band of the $e\,^1\Pi$–$a\,^1\Delta$ transition has been carried out and the molecular constants determined. The analysis of the previously observed $d\,^1\Sigma^+$–$X\,^3\Delta_1$ transition has also been extended by including the high J lines observed in our spectra. The present observations indicate that the $d\,^1\Sigma^+$ state of VN is affected by local perturbations in the $v = 2$ and 3 vibrational levels near $J' = 27$ and 20, respectively. The nature of the perturbing state could not be ascertained from our present observations and more experimental work is needed to draw a definite conclusion about the nature of the perturbing state (or states). Some additional *ab initio* predictions for the low-lying states would also be most welcome.

ACKNOWLEDGMENTS

We thank J. Wagner and C. Plymate of the National Solar Observatory for assistance in obtaining the spectra. The National Solar Observatory is operated by

the Association of Universities for Research in Astronomy, Inc., under contract with the National Science Foundation. The research described here was supported by funding from the NASA laboratory astrophysics program. Support was also provided by the Natural Sciences and Engineering Research Council of Canada.

REFERENCES

1. H. Spinard and R. F. Wing, *Annu. Rev. Astron. Astrophys.* **7,** 269–302 (1969).
2. F. A. Cotton, G. Wilkinson, C. A. Murillo, and M. Bochmann, "Advanced Inorganic Chemistry, A Comprehensive Text," 6th ed. Wiley, New York, 1999.
3. M. Grunze, *in* "The Chemical Physics of Solid Surfaces and Heterogeneous Catalysis" (D. A. King and D. P. Woodruf, Eds.), Vol. 4, p. 143. Elsevier, New York, 1982.
4. S. Ramanathan and S. T. Oyama, *J. Phys. Chem.* **99,** 16 365–16 372 (1995).
5. G. J. Leigh, *Science* **279,** 506–507 (1998).
6. Y. Nishibayashi, S. Iwai, and M. Hidai, *Science* **279,** 540–542 (1998).
7. C. Jascheck and M. Jascheck, "The Behavior of Chemical Elements in Stars." Cambridge Univ. Press, Cambridge, UK, 1995.
8. H. Machara and Y. Y. Yamashita, *Pub. Astron. Soc. Jpn.* **28,** 135–140 (1976).
9. D. L. Lambert and R. E. S. Clegg, *Mon. Not. R. Astron. Soc.* **191,** 367–389 (1980).
10. B. Lindgren and G. Olofsson, *Astron. Astrophys.* **84,** 300–303 (1980).
11. O. Engvold, H. Wöhl, and J. W. Brault, *Astron. Astrophys. Suppl. Ser.* **42,** 209–213 (1980).
12. K. L. Kunze and J. F. Harrison, *J. Am. Chem. Soc.* **112,** 3812–3625 (1990).
13. I. Shim and K. A. Gingerich, *Int. J. Quant. Chem.* **46,** 145–157 (1993).
14. C. W. Bauschlicher, Jr., *Chem. Phys. Lett.* **100,** 515–518 (1983).
15. S. M. Mattar, *J. Phys. Chem.* **97,** 3171–3175 (1993).
16. S. M. Mattar and B. J. Doleman, *Chem. Phys. Lett.* **216,** 369–374 (1993).
17. J. F. Harrison, *J. Phys. Chem.* **100,** 3513–3519 (1996).
18. P. E. M. Siegbahn and M. R. A. Blomberg, *Chem. Phys.* **87,** 189–201 (1984).
19. M. R. A. Blomberg and P. E. M. Siegbahn, *Theor. Chim. Acta* **81,** 365–374 (1992).
20. A. Fiedler and S. Twata, *Chem. Phys. Lett.* **271,** 143–151 (1997).
21. R. S. Ram, J. Liévin, and P. F. Bernath, *J. Chem. Phys.* **109,** 6329–6337 (1998).
22. R. S. Ram, J. Liévin, and P. F. Bernath, *J. Mol. Spectrosc.* **197,** 133–146 (1999).
23. R. S. Ram, J. Liévin, and P. F. Bernath, *J. Chem. Phys.* **111,** 3449–3456 (1999).
24. R. S. Ram and P. F. Bernath, *J. Chem. Phys.* **96,** 6344–6347 (1992).
25. R. S. Ram and P. F. Bernath, *J. Mol. Spectrosc.* **165,** 97–106 (1994).
26. R. S Ram and P. F. Bernath, *J. Mol. Spectrosc.* **184,** 401–412 (1997).
27. R. S. Ram and P. F. Bernath, *J. Opt. Soc. Am.* **11 B,** 225–230 (1994).
28. R. S. Ram, P. F. Bernath, W. J. Balfour, J. Cao, C. X. W. Qian, and S. J. Rixon, *J. Mol. Spectrosc.* **168,** 350–362 (1994).
29. W. J. Balfour, J. Cao, C. X. W. Qian, and S. J. Rixon, *J. Mol. Spectrosc.* **183,** 113–118 (1997).
30. W. J. Balfour, C. X. W. Qian, and C. Zhou, *J. Chem. Phys.* **106,** 4383–4388 (1997); **107,** 4473–4482 (1997).
31. E. J. Friedman-Hill and R. W. Field, *J. Chem. Phys.* **100,** 6141–6152 (1994).
32. A. J. Merer, G. Huang, A. S.-C. Cheung, and A. W. Taylor, *J. Mol. Spectrosc.* **125,** 465–503 (1987).
33. A. S.-C. Cheung, P. G. Hajigeorgiou, G. Huang, S.-Z. Huang, and A. J. Merer, *J. Mol. Spectrosc.* **163,** 443–458 (1994).
34. A. G. Adam, M. Barnes, B. Berno, R. D. Bower, and A. J. Merer, *J. Mol. Spectrosc.* **170,** 94–130 (1999).
35. S. L. Peter and T. M. Dunn, *J. Chem. Phys.* **90,** 5333–5336 (1989).
36. B. Simard, C. Masoni, and P. A. Hackett, *J. Mol. Spectrosc.* **136,** 44–55 (1989).
37. W. J. Balfour, A. J. Merer, H. Niki, B. Simard, and P. A. Hackett, *J. Chem. Phys.* **99,** 3288–3303 (1993).
38. R. S. Ram, P. F. Bernath, and S. P. Davis, *J. Chem. Phys.* **114,** 4457–4460 (2001).
39. L. Andrews, W. D. Bare, and G. V. Chertihin, *J. Phys. Chem. A* **101,** 8417–8427 (1997).
40. L. Andrews, *J. Elect. Spectrosc. Relate. Phenom.* **97,** 63–75 (1998).
41. T. C. Steimle, J. S. Robinson, and D. Goodridge, *J. Chem. Phys.* **110,** 881–889 (1999).
42. R. S. Ram, P. F. Bernath, S. P. Davis, and A. J. Merer, to be submitted.
43. A. G. Maki and J. S. Wells, "Wavenumber Calibration Tables from Heterodyne Frequency Measurements." NIST Special Publication 821, U.S. Government Printing Office, Washington, D.C., Dec. 1999.
44. L. A. Kaledin, J. E. McCord, and M. C. Heaven, *J. Mol. Spectrosc.* **173,** 499–509 (1995).
45. S. R. Langhoff, *Astrophys. J.* **481,** 1007–1015 (1997).
46. S. R. Langhoff and W. Bauschlicher, *J. Mol. Spectrosc.* **143,** 169–179 (1990).
47. Y. Azuma, G. Huang, M. P. J. Lyne, A. J. Merer, and V. I. Srdanov, *J. Chem. Phys.* **100,** 4138–4155 (1993).
48. R. S. Ram and P. F. Bernath, *J. Mol. Spectrosc.* **201,** 267–279 (2000).
49. A. J. Merer, A. S.-C. Cheung, and A. W. Taylor, *J. Mol. Spectrosc.* **108,** 343–351 (1984).